Available online at http://ijim.srbiau.ac.ir/
Int. J. Industrial Mathematics (ISSN 2008-5621)
Vol. 11, No. 1, 2019 Article ID IJIM-1232, 10 pages
Research Article

Mathematical Modeling of Micropolar Blood Flow in a Stenosed Artery Under the Body Acceleration and Magnetic Field

AR. Haghighi *†, N. Aliashrafi ‡, M. Kiyasatfar §

Received Date: 2017-12-28 Revised Date: 2018-09-21 Accepted Date: 2018-10-28

Abstract

This study aims to examine the pulsatile flow of blood through tapered artery with a stenosis under the effects of body acceleration and external magnetic field. Blood flow is modeled as non-Newtonian micropolar fluid. The non-linear governing equations of continuum and momentum in the cylindrical coordinate are being discretized using a finite difference approach and have been solved iteratively, through Crank-Nicolson method. The blood velocity distribution, volumetric flow rate and Resistance to blood flow at the stenosis throat are computed for various values of angle of tapering, amplitudes of body acceleration and Hartman number. It is shown that the results are in good agreement with the previous studies.

Keywords : Stenosed artery; Micropolar fluid; Body acceleration; Magnetic field; Crank-Nicolson method.

1 Introduction

Blocked blood vessels are cause of stroke and heart attack and in recent years scientists have focused on mathematical models of blood flow in stenosed Vessels to provide better therapies or help create more efficient medical equipments. Mathematical modeling of blood flow in the disease stenosis artery is very important due to considerable applications in medical and biomedical engineering. Hence, research on characteristic of blood flow in stenosis arteries has received great attention.

A large number of experimental and numerical studies that focus on blood flow behavior in artery with different shape of stenosis have been reported. However, most of them are limited to Newtonian fluids [1, 2, 3, 4]. Many biofluids such as blood are classified as non-Newtonian fluids, whose viscosities are basically a function of shear rate, different from those of Newtonian fluids. Recently, interest in problems of non-Newtonian fluid have grown and many mathematical models for describing the blood flow in artery by considering the rheological behavior of blood have been extensively developed [5, 6, 7, 8]. heological behavior of blood have been extensively developed. In these studies the non-Newtonian nature of blood are described by different models, such as

*Corresponding author. ah.haghighi@gmail.com, Tel:+98(918)3996782.
†Department of Mathematical, Technical and Vocational University, Tehran, Iran.
‡Department of Mathematics, Urmia University of Thechnology, Urmia, Iran.
§Faculty of Engineering, Urmia University, Urmia, Iran.

power law [9, 10], Sisko [11, 12, 13], Carreau [14] and micropolar [8, 15, 16]. In addition to considering the blood non-Newtonian rheology, the micropolar model takes care the effect of microrotations of microelements suspended in plasma by using of independent microrotation vector.

Due to electrical conductivity of blood, the externally applied magnetic field effects on blood flow in arteries and changes the velocity profiles. This physical phenomena can be very useful in diagnosis and treatment of vascular diseases. Several works in which the effect of MHD on characteristic of flow for various models of blood and stenosed artery geometries are investigated have been documented in [14, 17, 18, 19, 20, 21].

Patients with blocked vessels, when exposed to body acceleration, like shaking when driving vehicles or flying in an airplane, and fast body exercises, causes serious physical problems such as headaches, loss of vision, increased heart rate and bleeding in Face, neck and brain. Body acceleration highly influenced the blood velocity, shear stress, flow rate and impedance in a blocked artery. Due to these physiological importance of body acceleration, research in this area has intensified recently and many works have been reported [23, 24, 25].

A review of previous works show that the investigation of micropolar blood flow through tapered stenosed artery subjected to external magnetic field and body acceleration has received little attention. Motivated by this, the main aim of this work is to investigate the effects of external magnetic field and body acceleration on blood pulsatile flow in tapered stenosed artery with emphasis on micropolar nature of blood using implicit finite difference Crank-Nicolson method.

2 Mathematical Equations

Consider a two-dimensional, unsteady, fully developed and axially symmetric flow of blood and also, the fluid blood is assumed to behave like a micropolar fluid. Let (r, θ, z) be the cylindrical polar coordinats system, in which r and z axes are the radial and axial directions of the artery. v_1, v_2 and v_3 are the axial, radial and microrotational velocity components respectively. The blood flow in a vibration environmental is considered, in which exist the acceleration. Also, the magnetic field strength $B = (B_0 + B_1)$ applied for the flow of blood. The governing equations for micropolar fluid may be written in non-dimensional forms as follows:

$$\frac{\partial v_1}{\partial z} + \frac{\partial v_2}{\partial r} + \frac{v_2}{r} = 0, \tag{2.1}$$

$$\frac{\partial v_1}{\partial t} + v_2\frac{\partial v_1}{\partial r} + v_1\frac{\partial v_1}{\partial z} = -\frac{\partial p}{\partial z} + \frac{1}{Re}\left(\frac{\partial^2 v_1}{\partial r^2} + \frac{1}{r}\frac{\partial v_1}{\partial r} + \frac{\partial^2 v_1}{\partial z^2}\right) + \frac{m}{Re}\left(\frac{\partial v_3}{\partial r} + \frac{v_3}{r}\right) - \frac{1}{Re}Ha^2 v_1 + \frac{1}{Re}G(t), \tag{2.2}$$

$$\frac{\partial v_2}{\partial t} + v_2\frac{\partial v_2}{\partial r} + v_1\frac{\partial v_2}{\partial z} = -\frac{\partial p}{\partial r} + \frac{1}{Re}\left(\frac{\partial^2 v_2}{\partial r^2} + \frac{1}{r}\frac{\partial v_2}{\partial r} + \frac{\partial^2 v_2}{\partial z^2} - \frac{v_2}{r^2}\right) + \frac{m}{Re}\left(\frac{\partial v_3}{\partial z}\right), \tag{2.3}$$

$$\frac{JM}{1-m}\left(\frac{\partial v_3}{\partial t} + v_2\frac{\partial v_3}{\partial r} + v_1\frac{\partial v_3}{\partial z}\right) = -\frac{2N}{Re}v_3 + \frac{N}{Re}\left(\frac{\partial v_2}{\partial z} - \frac{\partial v_1}{\partial r}\right) + \frac{1}{Re}\left(\frac{\partial^2 v_3}{\partial r^2} + \frac{1}{r}\frac{\partial v_3}{\partial r} + \frac{\partial^2 v_3}{\partial z^2} - \frac{v_3}{r^2}\right). \tag{2.4}$$

The dimensionless pressure gradient and the body acceleration respectively, can be written as [4, 3, 12, 26]:

$$-\frac{\partial p}{\partial z} = A_0 + A_1 cos\omega t, \quad t > 0, \tag{2.5}$$

$$G(t) = a_0 cos(bt + \varphi_g). \tag{2.6}$$

where $a_0 = \frac{a^2 a_0^*}{\nu U}$, $b = \frac{w_b}{w}$, A_0 is the constant amplitude of the pressure gradient, A_1 is the amplitude of the pulsatile component giving rise to

systolic and diastolic pressures, $w = 2\pi f_p$, f_p being the pulse frequency.

The following non-dimensional quantities have been used in Eqs. (2.1)-(2.4):

$$v_1 = \frac{v_1^*}{U}, v_2 = \frac{v_2^*}{U}, r = \frac{r^*}{a}, v_3 = \frac{av_3^*}{a}, z = \frac{z^*}{a},$$
$$t = \frac{t^*U}{a}, J = \frac{J^*}{a^2}, p = \frac{p^*}{\rho U^2}, Re = \frac{\rho U a}{\mu + k},$$
$$N = \frac{\kappa a^2}{\nu}, M = \frac{\mu a^2}{\nu}, m = \frac{\kappa}{\mu + \kappa}.$$

where p is the pressure, ρ is the density, J is the microinertia constant, μ is the viscosity, κ is the rotational viscosity, ν is the material constant and $Ha = B_0 a\sqrt{\frac{\sigma}{\rho\nu}}$ is the Hartmann number.

The initially and boundary conditions are as follows [27, 28] :

$$r = 0 : \quad \frac{\partial v_1(r,z,t)}{\partial r} = 0,$$
$$v_2(r,z,t) = v_3(r,z,t) = 0, \tag{2.7}$$

$$r = R(z) : \quad v_1(r,z,t) = 0,$$
$$v_2(r,z,t) = \frac{\partial R}{\partial t}, v_3(r,z,t) = -\lambda\frac{\partial v_1}{\partial r} \tag{2.8}$$

$$v_1(r,z,0) =$$
$$2\overline{v_1}[1-(\frac{r}{R})^2+\frac{4\gamma}{\beta^2}I_0(\beta)\frac{I_0(\frac{\beta r}{R})}{I_0(\beta)} - 1],$$
$$v_2(r,z,0) = v_3(r,z,0) = 0. \tag{2.9}$$

where $\gamma = \frac{m\beta}{4I_0(\beta)}$, $\beta^2 = N(2-m)$. $\overline{v_1}$ is the mean axial velocity at any given cross-section. I_0 is the modified Bessel functions of zeroth-order of first kind.

The geometry of the time variant stenosis is constructed mathematically in non-dimensional form as (see Fig. 1) [7, 29, 30]:

$$R(z,t) = \begin{cases} [(mz+a) + \frac{\tau_m sec\psi(z-\psi)}{\tau_m^2 sin\psi^2 - \frac{l_0^2}{4}} \\ (l_0 - (z-d_1))]a_1(t) \quad d_1 \le z \le d_1 l_0 \\ \\ (mz+a)a_1(t) \qquad otherwise \end{cases} \tag{2.10}$$

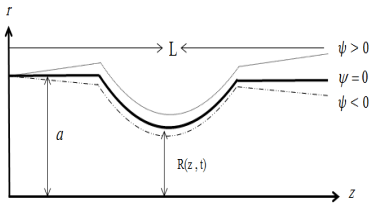

Figure 1: Geometry of the stenosed artery.

In above expression, $R(z,t)$ represents the radius of the arterial segment in the constricted region, ψ is the angle of tapering, a is the radius of the artery in the non-stenotic region, d_1 is location of the stenosis, L is the finite length of arterial segment. The time-variant parameter $a_1(t)$ is given by $a_1(t) = 1 - b(cos\omega t - 1)e^{-b\omega t}$ [12, 29, 30, 31], in which b is a constant, $w = 2\pi f_p$, f_p is the pulse frequency.

3 Method of solution

We introduce a suitable coordinate transformation by $\eta = \frac{r}{R}$ [7, 10, 12, 32, 33, 34] for the purpose of prove the artery wall. By using this transformation Eqs. (2.1-2.4 and 2.7-2.9) take the following form:

$$\frac{\partial v_1}{\partial t} = -\frac{\partial p}{\partial z}+\frac{1}{R}\frac{\partial v_1}{\partial \eta}\left[\eta\left(v_1\frac{\partial R}{\partial z}+\frac{\partial R}{\partial t}\right)-v_2\right]-v_1\frac{\partial v_1}{\partial z}$$
$$+\frac{1}{Re}\left[\frac{1}{R^2}\left\{1+(\eta\frac{\partial R}{\partial z})^2\right\}\frac{\partial^2 v_1}{\partial \eta^2}+\frac{1}{\eta R^2}\left\{1+2(\eta\frac{\partial R}{\partial z})^2\right.\right.$$
$$\left.\left.-\eta^2 R\frac{\partial^2 R}{\partial z^2}\right\}\frac{\partial v_1}{\partial \eta}+\frac{\partial^2 v_1}{\partial z^2}\right]+\frac{m}{Re}(\frac{1}{R}\frac{\partial v_3}{\partial \eta}+\frac{v_3}{\eta R})$$
$$-\frac{1}{Re}Ha^2 v_1 + \frac{1}{Re}G(t), \tag{3.11}$$

$$\frac{\partial v_3}{\partial t} = \frac{1}{R}\frac{\partial v_3}{\partial \eta}\left[\eta\left(v_1\frac{\partial R}{\partial z}+\frac{\partial R}{\partial t}\right)-v_2\right]-v_1\frac{\partial v_3}{\partial z}$$
$$+\frac{1-m}{MReJ}\left[N(-2v_3+\frac{\partial v_2}{\partial z}-\frac{\eta}{R}\frac{\partial R}{\partial z}\frac{\partial v_2}{\partial \eta}-\frac{1}{R}\frac{\partial v_1}{\partial \eta})\right.$$
$$+\left\{\frac{1}{R^2}(1+(\eta\frac{\partial R}{\partial z})^2)\frac{\partial^2 v_3}{\partial \eta^2}+\frac{1}{\eta R^2}\left\{1+2(\eta\frac{\partial R}{\partial z})^2\right.\right.$$

$$-\eta^2 R\frac{\partial^2 R}{\partial z^2}\Big\}\times\frac{\partial v_3}{\partial \eta}+\frac{\partial^2 v_3}{\partial z^2}-\frac{v_3}{(\eta R)^2}\Big\}\Big], \quad (3.12)$$

$$\frac{1}{R}\frac{\partial v_2}{\partial \eta}+\frac{v_2}{\eta R}+\frac{\partial v_1}{\partial z}-\frac{\eta}{R}\frac{\partial R}{\partial z}\frac{\partial v_1}{\partial \eta}=0, \quad (3.13)$$

The initially and boundary conditions are:

$$\eta=0: \quad \frac{\partial v_1(\eta,z,t)}{\partial \eta}=0, v_2(\eta,z,t)=0,$$
$$v_3(\eta,z,t)=0, \quad (3.14)$$
$$\eta=1: \quad v_1(\eta,z,t)=0, v_2(\eta,z,t)=\frac{\partial R}{\partial t},$$
$$v_3(\eta,z,t)=-\frac{\lambda}{R}\frac{\partial v_1}{\partial \eta}, \quad (3.15)$$
$$v_1(\eta,z,0)=2\overline{v_1}[1-\eta^2+\frac{4\gamma}{\beta^2}I_0(\beta)\{\frac{I_0(\beta\eta)}{I_0(\beta)}\}-1],$$
$$v_2(\eta,z,0)=v_3(\eta,z,0)=0. \quad (3.16)$$

For compute the radial velocity component by using the continuity equation. Thus, multiply Eq. (3.13) by ηR and integrate with respect to η in the interval of $[0,\ \eta]$, arrive:

$$\eta v_1(\eta,z,t)+R\int_0^\eta \eta\frac{\partial v_1}{\partial z}d\eta-\frac{\partial R}{\partial z}\eta^2 v_1$$
$$+\frac{\partial R}{\partial z}\int_0^\eta 2\eta v_1 d\eta=0 \quad (3.17)$$

Applying the boundary condition $\eta=1$, Eq. (3.17) yields:

$$\int_0^1 \eta\frac{\partial v_1}{\partial z}d\eta=-\int_0^1 \frac{2}{R}\frac{\partial R}{\partial z}\eta v_1 d\eta$$
$$+\int_0^1 \frac{1}{R}(\frac{\partial R}{\partial t}\eta f(\eta))d\eta. \quad (3.18)$$

Now choose $f(\eta)=4(1-\eta^2)$, that is satisfied $\int_0^1 \eta f(\eta)d\eta=1$. Taking integrating of both sides Eq. (3.18) can be written as:

$$\frac{\partial v_1}{\partial z}=-\frac{2}{R}\frac{\partial R}{\partial z}v_1-\frac{4}{R}(1-\eta^2)\frac{\partial R}{\partial t}. \quad (3.19)$$

Substituting (3.19) into (3.17), the radial velocity component can be obtained as follows:

$$v_2(\eta,z,t)=\eta[\frac{\partial R}{\partial z}v_1+\frac{\partial R}{\partial t}(2-\eta^2)]. \quad (3.20)$$

4 Computational Scheme

For compute the axial velocity component by applying Crank-Nicolson method. In this method, all the spatial derivatived and all the time derivatives discretized by using central difference formula and forward difference formula respectively. So, the spatial derivatived and the time derivatives as following:

$$\frac{\partial v_1}{\partial \eta}=\frac{1}{2}[\frac{(v_1)^k_{i,j+1}-(v_1)^k_{i,j-1}}{2\Delta\eta}+$$
$$+\frac{(v_1)^{k+1}_{i,j+1}-(v_1)^{k+1}_{i,j-1}}{2\Delta\eta}], \quad (4.21)$$

$$\frac{\partial v_1}{\partial z}=\frac{(v_1)^k_{i+1,j}-(v_1)^k_{i-1,j}}{2\Delta z}, \quad (4.22)$$

$$\frac{\partial^2 v_1}{\partial \eta^2}=\frac{1}{2}[\frac{(v_1)^k_{i,j+1}-2(v_1)^k_{i,j}+(v_1)^k_{i,j-1}}{\Delta\eta^2}$$
$$+\frac{(v_1)^{k+1}_{i,j+1}-2(v_1)^{k+1}_{i,j}+(v_1)^{k+1}_{i,j-1}}{\Delta\eta^2}], \quad (4.23)$$

$$\frac{\partial^2 v_1}{\partial z^2}=\frac{(v_1)^k_{i+1,j}-2(v_1)^k_{i,j}+(v_1)^k_{i-1,j}}{\Delta z^2}, \quad (4.24)$$

$$\frac{\partial v_1}{\partial t}=\frac{(v_1)^{k+1}_{i,j}-(v_1)^k_{i,j}}{\Delta t}. \quad (4.25)$$

Using these methode, the discretized form of Eqs. (3.11) and (3.12) can be written as:

$$A_{i,j}(v_1)^{k+1}_{i,j-1}+B_{i,j}(v_1)^{k+1}_{i,j}+C_{i,j}(v_1)^{k+1}_{i,j+1}$$
$$=D_{i,j}, \quad (4.26)$$

$$A_{i,j}=\frac{\Delta t}{4R^k_i\Delta\eta}[\eta_j((v_1)_{i,j}(\frac{\partial R}{\partial z})^k_i+(\frac{\partial R}{\partial t})^k_i)$$
$$-(v_2)_{i,j}]-\frac{\Delta t}{2Re(R^k_i)^2\Delta\eta^2}\{1+(\eta_j(\frac{\partial R}{\partial z})^k_i)^2\}$$

$$+\frac{\Delta t}{4Re(R_i^k)^2\eta_j\Delta\eta}\{1+2(\eta_j(\frac{\partial R}{\partial z})_i^k)^2$$
$$-\eta_j^2R_i^k(\frac{\partial^2R}{\partial z^2})_i^k\},$$
$$B_{i,j}=1+\frac{\Delta t}{Re(R_i^k)^2\Delta\eta^2}\{1+(\eta_j(\frac{\partial R}{\partial z})_i^k)^2\},$$

$$C_{i,j}=\frac{-\Delta t}{4R_i^k\Delta\eta}[\eta_j((v_1)_{i,j}(\frac{\partial R}{\partial z})_i^k+(\frac{\partial R}{\partial t})_i^k)$$
$$-(v_2)_{i,j}]-\frac{\Delta t}{2Re(R_i^k)^2\Delta\eta^2}\{1+(\eta_j(\frac{\partial R}{\partial z})_i^k)^2\}$$
$$-\frac{\Delta t}{4(R_i^k)^2\eta_j\Delta\eta}\{1+2(\eta_j(\frac{\partial R}{\partial z})_i^k)^2$$
$$-\eta_j^2R_i^k(\frac{\partial^2R}{\partial z^2})_i^k\},$$

$$D_{i,j}=(v_1)_{i,j}^k-\Delta t(\tfrac{\partial P}{\partial z})$$
$$+\frac{\Delta t}{4R_i^k\Delta\eta}((v_1)_{i,j+1}^k-(v_1)_{i,j-1}^k)$$
$$[\eta_j((v_1)_{i,j}(\frac{\partial R}{\partial z})_i^k+(\frac{\partial R}{\partial t})_i^k)-(v_2)_{i,j}]$$
$$-\frac{\Delta t}{2\Delta z}(v_1)_{i,j}^k((v_1)_{i+1,j}^k-(v_1)_{i-1,j}^k)$$
$$+\frac{\Delta t}{2Re(R_i^k)^2\Delta\eta^2}((v_1)_{i,j+1}^k-2(v_1)_{i,j}^k$$
$$+(v_1)_{i,j-1}^k)\{1+(\eta_j(\frac{\partial R}{\partial z})_i^k)^2\}$$
$$+\frac{\Delta t}{4Re(R_i^k)^2\eta_j\Delta\eta}\{1+2(\eta_j(\frac{\partial R}{\partial z})_i^k)^2$$
$$-\eta_j^2R_i^k(\frac{\partial^2R}{\partial z^2})_i^k\}((v_1)_{i,j+1}^k-(v_1)_{i,j-1}^k)$$
$$+\frac{\Delta t}{Re\Delta z^2}((v_1)_{i+1,j}^k-2(v_1)_{i,j}^k+(v_1)_{i-1,j}^k)$$
$$+\Delta t[\frac{m}{Re}(\frac{1}{R_i^k}(\frac{(v_3)_{i,j+1}^k-(v_3)_{i,j-1}^k}{2\Delta\eta})+\frac{(v_3)_{i,j}}{\eta_jR_i^k})]$$
$$-\Delta t(\frac{Ha^2}{Re})v_1+\frac{\Delta t}{Re}G(t).$$

and

$$E_{i,j}(v_3)_{i,j-1}^{k+1}+F_{i,j}(v_3)_{i,j}^{k+1}+G_{i,j}(v_3)_{i,j+1}^{k+1}$$
$$=H_{i,j},\qquad(4.27)$$

$$E_{i,j}=\frac{\Delta t}{4R_i^k\Delta\eta}[\eta_j((v_1)_{i,j}(\frac{\partial R}{\partial z})_i^k+(\frac{\partial R}{\partial t})_i^k)-(v_2)_{i,j}]$$
$$-\frac{\Delta t(1-m)}{2ReMJ(R_i^k)^2\Delta\eta^2}\{1+(\eta_j(\frac{\partial R}{\partial z})_i^k)^2\}$$
$$+\frac{\Delta t(1-m)}{4ReMJ(R_i^k)^2\eta_j\Delta\eta}$$
$$\{1+2(\eta_j(\tfrac{\partial R}{\partial z})_i^k)^2-\eta_j^2R_i^k(\tfrac{\partial^2R}{\partial z^2})_i^k\},$$
$$F_{i,j}=1+\frac{\Delta t(1-m)}{ReJM(R_i^k)^2\Delta\eta^2}\{1+(\eta_j(\frac{\partial R}{\partial z})_i^k)^2\},$$

$$G_{i,j}=\frac{-\Delta t}{4R_i^k\Delta\eta}[\eta_j((v_1)_{i,j}(\frac{\partial R}{\partial z})_i^k+(\frac{\partial R}{\partial t})_i^k)$$
$$-(v_2)_{i,j}]-\frac{\Delta t(1-m)}{2ReJM(R_i^k)^2\Delta\eta^2}$$
$$\{1+(\eta_j(\frac{\partial R}{\partial z})_i^k)^2\}-\frac{\Delta t(1-m)}{4ReJM(R_i^k)^2\eta_j\Delta\eta}$$
$$\{1+2(\eta_j(\frac{\partial R}{\partial z})_i^k)^2-\eta_j^2R_j^k(\frac{\partial^2R}{\partial z^2})_i^k\},$$

$$H_{i,j}=(v_3)_{i,j}^k+\frac{\Delta t}{4R_i^k\Delta\eta}((v_3)_{i,j+1}^k-(v_3)_{i,j-1}^k)$$
$$[\eta_j((v_1)_{i,j}(\frac{\partial R}{\partial z})_i^k+(\frac{\partial R}{\partial t})_i^k)-(v_2)_{i,j}]$$
$$-\frac{\Delta t}{2\Delta z}(v_1)_{i,j}^k((v_3)_{i+1,j}^k-(v_3)_{i-1,j}^k)$$
$$+\frac{\Delta tN(1-m)}{ReMJ}(-2(v_3)_{i,j}$$
$$+(\frac{(v_2)_{i+1,j}^k-(v_2)_{i-1,j}^k}{2\Delta z})-\frac{\eta_j}{R_i^k}(\frac{\partial R}{\partial z})_i^k$$
$$(\frac{(v_2)_{i,j+1}^k-(v_2)_{i,j-1}^k}{2\Delta\eta})$$
$$-\frac{1}{R_i^k}(\frac{(v_1)_{i,j+1}^k-(v_1)_{i,j-1}^k}{2\Delta\eta}))$$
$$+\frac{\Delta t(1-m)}{2MReJ(R_i^k)^2\Delta\eta^2}(1+(\eta_j(\frac{\partial R}{\partial z})_i^k)^2)$$
$$((v_3)_{i,j+1}^k-2(v_3)_{i,j}^k+(v_3)_{i,j-1}^k)$$
$$+\frac{\Delta t(1-m)}{4MReJ\eta_j(R_i^k)^2\Delta\eta}((v_3)_{i,j+1}^k-(v_3)_{i,j-1}^k)$$

$$\{1+2(\eta_j(\frac{\partial R}{\partial z})_i^k)^2-\eta_j^2 R_i^k(\frac{\partial^2 R}{\partial z^2})_i^k\}$$
$$+\frac{\Delta t(1-m)}{\Delta z^2 MReJ}((v_3)_{i+1,j}^k-2(v_3)_{i,j}^k+(v_3)_{i-1,j}^k)$$
$$-\frac{\Delta t(1-m)(v_3)_{i,j}}{MReJ(\eta_j R_i^k)^2}.$$

The rate of flow (Q) and the resistive impedance (Λ) in non-dimensional forms can be obtained:

$$Q_i^k = 2\pi(R_i^k)^2\int_0^1 \eta_j(v_1)_{i,j}^k d\eta_j, \tag{4.28}$$

$$\Lambda_i^k = \frac{|L(\frac{\partial p}{\partial z})_i^k|}{Q_i^k}. \tag{4.29}$$

5 Results and discussion

Numerical computations have been carried out by using the following data [29, 35, 36]:

$$\Delta t = 0.001, \Delta\eta = 0.125, \Delta z = 0.1, d = 10,$$
$$Re = 300, L = 45, a = 1.52, A_0 = 0.1,$$
$$A_1 = 0.2A_0, N = 1, M = 1,$$
$$m = 0.85, f_p = 1.2.$$

In order to verify the numerical method proposed in this paper, the present numerical results are compared with the results by Ponalagusamy and Priyadharshini [37] for velocity distribution in the case of micropolar fluid. The comparisons are shown in Fig. 2. As it can be seen, there is agreement between them. Figure 3 shows the axial velocity profiles of micropolar fluid through a stenosed artery, at the specific location $z = 28$ at $t = 9$ and $\tau_m = 0.2a$, for different values of Hartmann number. As expected because of Lorentz forces effect, by increasing the Hartman number the maximum axial velocity decreases. As a consequence, under the action of a magnetic field, the volume of blood flow can be controlled during surgeries. Figure 4 depicts the effects of Hartman number and the amplitudes of body acceleration on microrotational velocity at the time $t = 8$ and $t = 4$ in maximum constricted region. It is observed that the microrotational velocity decreases with the increase of the Hartmann number and increases with the increases of the amplitudes of body. The rate of flow in the stenosed artery for different Hartmann number at the $t = 4$ and $\tau_m = 0.2a$ is shown in Fig. 5. Considering Eq. (4.28) the rate of flow and the axial velocity profile are directly related. so the rate of flow decreases with hartman number due to decreasing of axial mean velocity. Figure 6 illustrates the rate of flow for different amplitudes of body acceleration at the time $t = 4$ and $\tau_m = 0.2a$. In Fig. 6, it is shown that by increasing the amplitute of body acceleration, the flow rate increases. So, the blood flow may increases in the vibration environmental. The resistive impedance in the stenosed artery for the different Hartmann number at the time $t = 4$ and $\tau_m = 0.2a$ is obvious in Fig. 7. Considering Eq. (4.29) the rate of flow and the resistive impedance are inversely related

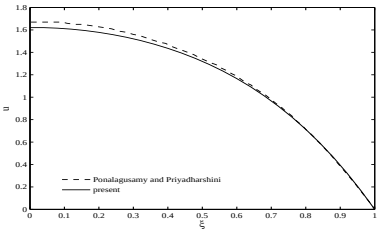

Figure 2: Comparison of the dimensionless axial velocity profile.

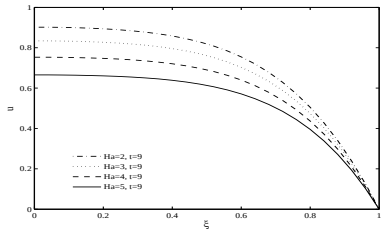

Figure 3: The axial velocity profiles for different Hartmann number.

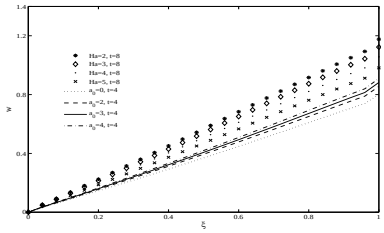

Figure 4: The microrotational velocity profiles for different amplitudes of body acceleration and Hartmann number.

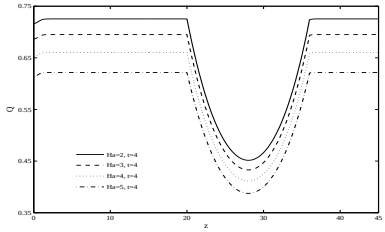

Figure 5: Distribution of the rate of flow for different Hartmann number.

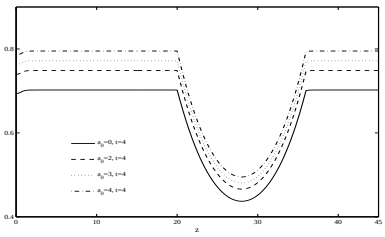

Figure 6: Distribution of the rate of flow for different amplitudes of body acceleration.

so, unlike the rate of flow, the resistive impedance increases with the increase in the Hartmann number. Resistive impedance through a stenosed

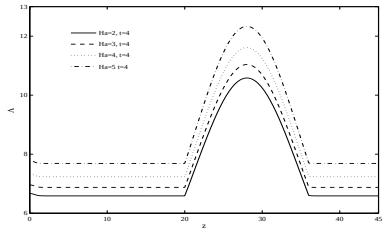

Figure 7: Distribution of the resistive impedance for different Hartmann number.

artery for different amplitudes of body acceleration at the time $t = 4$ is presented in Fig. 8. As shown, the resistive impedance decreases with the increase in the amplitudes of body acceleration. Fig. 9 depicts the blood flow patterns for different values of tapering angle and stenosis size. Panels (a) and (b) show flow pattern for the stenosis artery. Obviosly, increasing the size of stenosis at t=4 leads to the decrease of the flow lines, thus, increasing the size of stenosis gives rise to the decrease of the axial velocity. Panel (c) describes the flow lines for the converging stenosis artery ($\psi > 0$). On the contrary panel (d) shows the diverging stenosis artery ($\psi < 0$) that decreases the flow lines with the decrease the tapering angle. So, the axial velocity decrease with decreases

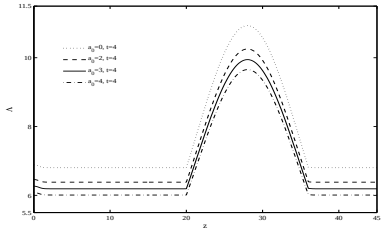

Figure 8: Distribution of the resistive impedance for different amplitudes of body acceleration.

of the taper angle at t=4.

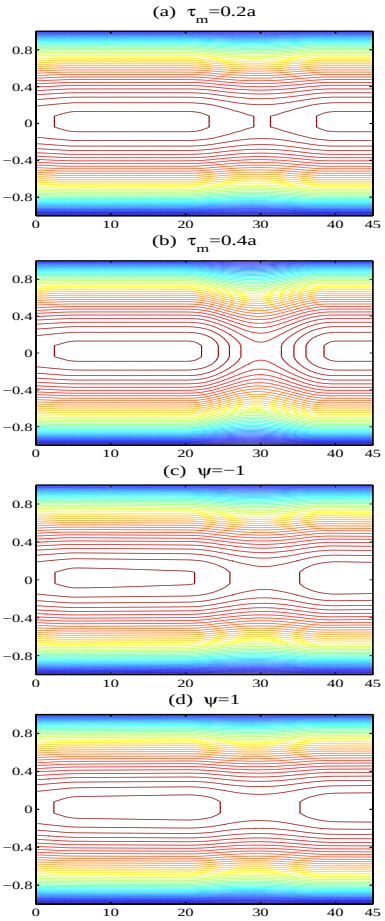

Figure 9: Instantaneous flow patterns of streaming blood

6 Conclusion

The pulsatile flow of conducting micropolar blood in a stenosed tapered artery under the influence of an applied external magnetic field and body acceleration numerically are studied using an implicit finite difference Crank-Nicolson method.

The results show that by increasing both taper angle and Hartman number. axial velocity and flow rate increase and in opposite trend, the resistive impedance and microrotational velocity decrease. Also, it is clear that as body acceleration increases, the axial velocity increases which leads to increase the of flow rate.

References

[1] Q. Long, X. Xu, K. Ramnarine and P. Hoskins, Numerical investigation of physiologically realistic pulsatile flow through arterial stenosis,*J. Biomech.* 34 (2001) 1229-1242.

[2] G. T. Liu, X. J. Wang, B. Q. Ai, L. G. Liu, Numerical study of pulsating flow through a tapered artery with stenosis, *Chinese. J. Phys.* 42 (2004) 401-409.

[3] A. R. Haghighi, M. S. Asl, M. Kiyasatfar, Mathematical modeling of unsteady blood flow through elastic tapered artery with overlapping stenosed,*Journal of the Braziliam Society of Mechanical Sciences and Engineering* (2014).

[4] G. C. Shit, Sreeparna Majee, Pulsatile flow of blood and heat transfer with variable viscosity under magnetic and vibration environment, *Journal of Magnetism and Magnetic Materials* 388 (2015) 106-115.

[5] H. Jung, J. W. Choi, C. G. Park, Asymmetric flows of non-Newtonian fluids in symmetric stenosed artery, *Korea Aust. Rheol. J.* 16 (2004) 101-108.

[6] D. Sankar, K. Hemalatha, A non-Newtonian fluid flow model for blood flow through a catheterized artery Steady flow, *Appl. Math. Model.* 31 (2007) 1847-1864.

[7] D. Sankar, U. Lee, FDM analysis for MHD flow of a non-Newtonian fluid for blood flow in stenosed arteries, *J. Mech. Sci. Technol.* 25 (2011) 2573-2581.

[8] D. Srikanth, K. Taddesse, Mathematical analysis of non-Newtonian fluid flow through multiple stenotic artery in the presence of cathetera pulsatile flow, *Int. J. Nonlinear Sci.* 13 (2012) 15-27.

[9] P. K. Mandal, An unsteady analysis of non-Newtonian blood flow through tapered arteries with a stenosis, *Internat. J. Non-Linear Mech.* 40 (2005) 151-164.

[10] Md. A. Ikbal, , S. Chakravarty, Kelvin K. L. Wong, J. Mazumdar, P. K. Mandal, Unsteady response of Non-Newtonian blood flow through a stenosed artery in magnetic field, *Comput. Appl. Math.* 230 (2009) 243-259.

[11] AR. Haghighi, S. Asadi chalak, Mathematical modelling of Sisko fluid flow through a stenosed artery, *International Journal of Industrial Mathematics* 9 (2017) 12-31.

[12] N. Ali, A. Zaman, M. Sajid, Unsteady blood flow through a tapered stenotic artery using Sisko model, *Computers and Fluids* 101 (2014) 42-49.

[13] AR. Haghighi, S. Asadi chalak, Mathematical modeling of blood flow through a stenosed artery under body acceleration, *Journal of the Brazilian Society of Mechanical Sciences and Engineering* 39 (2017) 2487-2494.

[14] N. Ali, A. Zaman, M. Sajid, J. J. Nieto, A. Torres, Unsteady non-Newtonian blood flow through a tapered overlapping stenosed catheterized vesse, *Mathematical Biosciences*, (2015).

[15] A. Ilyani, A. Norsarahaida, A micropolar fluid model of blood flow through a tapered artery with a stenosis, *Math. Meth. Appl. Sci.* 33 (2010) 1910-1923.

[16] A. Zaman, N. Ali, O. Anwar Bg, Numerical simulation of unsteady micropolar hemodynamics in a tapered catheterized artery with a combination of stenosis and aneurysm, *Med Biol Eng Comput,* (2015).

[17] AR Haghighi, R. N Pralhad, Mathematical modelling of blood flows under the effects of body forces and magnetism on human body,

International Journal of Biomedical Engineering and Technology 2 (2015) 295-303.

[18] Kh. S. Mekheimer, Mohammed H. Haroun, M. A. El Kot, Induced magnetic field influences on blood flow through an anisotropically tapered elastic artery with overlapping stenosis in an annulus, *Can. J. Phys.* 89 (2011) 201-212.

[19] D. Srikanth, J. V. Ramana Reddy, Shubha Jain, Anup Kale, Unsteady polar fluid model of blood flow through tapered x-shape stenosed artery: Effects of catheter and velocity slip, *Ain Shams Engineering Journal* (2015).

[20] T. Hayat, Taseer Muhammad, S. A. Shehzad, A. Alsaedi, On three-dimensional boundary layer flow of Sisko nanofluid with magnetic field effects, *Advanced Powder Technology,* (2016).

[21] AR. Haghighi, N. Aliashrafi, A mathematical modeling of pulsatile blood flow through a stenosed artery under effect of a magnetic field, *Journal of Mathematical Modeling* 6 (2018) 149-164.

[22] H. Jung, J. W. Choi, C. G. Park, Asymmetric flows of non-Newtonian fluids in symmetric stenosed artery, *Korea Aust. Rheol. J.* 16 (2004) 101-108.

[23] D. S. Shankar, U. Lee, Nonlinear mathematical analysis for blood flow in a constricted artery under periodic body acceleration, *Commun. Nonlinear Sci. Numer. Simulat.* 16 (2011) 4390-4402.

[24] A. Zaman, N. Ali, OA. Beg, Numerical study of unsteady blood flow through a vessel using Sisko model, *Int. J. Eng. Sci. Technol.* 19 (2015) 538-547.

[25] AR. Haghighi, N. Aliashrafi, N. Asghary, An implicit finite difference scheme for analyzing the effect of body acceleration on pulsatile blood flow through a stenosed artery, *Journal of Linear and Topological Algebra* 6 (2017) 147- 161.

[26] M. Massoudi, T. X. Phuoc, Pulsatile Flow of a blood using a modified second grade fluid model, *Compu. Math. Appl.* 56 (2008) 199-211.

[27] R. Devanathan, S. Parvathamma, Flow of micropolar fluid through a tube with stenosis, *Med. Biol. Engrg. Comput.* 21 (1983) 438-445.

[28] AR. Haghighi, Mathematical model of the impact of pressure drop on human body, *Selcuk Journal of Applied Mathematics* 13 (2012) 35-40.

[29] A. Zaman, N. Ali, M. Sajad, T. Hayat, Effects of unsteadiness and non-Newtonian rheology on blood flow through a tapered time-variant stenotic artery, *AIP Adv* 5 (2015) 37-42.

[30] N. Yamaguchi, Existence of global strong solution to the micropolar fluid system in a bounded domain, *Math Meth Appl Sci* 28 (2005) 1507-1526.

[31] AR. Haghighi, M. S. Asl, Mathematical modeling of micropolar fluid flow through an overlapping arterial stenosis, *International Journal of Biomathematics* 8 (2015) 11-18.

[32] S. Chakravarty, P. K. Mandal, Unsteady flow of a two-layer bloodstream past a tapered flexible artery under stenotic conditions, *Comput. Meth. Appl. Math.* 4 (2004) 391-409.

[33] Z. Ismail, I. Abdullah, N. Mustapha, N. Amin, A power-law model of blood flow through a tapered overlapping stenosed artery, *Appl. Math. Comput.* 195 (2008) 669-680.

[34] AR. Haghighi, N. Aliashrafi, Mathematical modeling of pulsatile blood flow and heat transfer under magnetic and vibrating environment, *International Journal of Heat and Technology.* 36 (2018) 783-790.

[35] G. Bugliarello, J. Sevilla, Velocity distribution and other characteristics of steady and pulsatile blood flow in fine glass tubes, *Biorheology* 7 (1970) 85-93.

[36] P. Chaturani, V. Upadhya, On micropolar fluid model for blood flow through narrow tubes, *Biorheology* 16 (1979) 419-433.

[37] R. Ponalagusamy, S. Priyadharshini, Numerical investigation on two-fluid model (micropolar-Newtonian) for pulsatile flow of blood in a tapered arterial stenosis with radially variable magnetic field and core fluid viscosity, *Comp. Appl. Math.* (2016).

Ahmad Reza Haghighi is an Associate Professor in the department of mathematics at Technical and Vocational University(TVU), Tehran, Iran. He completed his Ph. D degree in applied mathematics from Pune University, India. His research interest includes Bio-Mathematics, Computational Fluid Dynamics, numerical solution of functional equations, Partial Differential Equations and Control.

Nooshin Aliashrafi was born in Urmia, Iran. She received her B.Sc. degree in pure mathematics from University of Urmia. Also, she holds master degree in applied mathematics from Urmia University of Technology, Urmia, Iran. Her research areas include Bio-Mathematics, Numerical analysis, Partial Differential Equations.

Mehdi Kiyasatfar completed his Ph. D degree in the Department of Mechanical Engineering Urmia University of Technology, Urmia, Iran. His research interest includes Computational fluid dynamics (CFD).